



HAL
open science

Strain-induced resistance change in V_2O_3 films on piezoelectric ceramic disks

Joe Sakai, Maxime Bavencoffe, Béatrice Negulescu, Patrice Limelette, Jérôme Wolfman, Akinori Tateyama, Hiroshi Funakubo

► **To cite this version:**

Joe Sakai, Maxime Bavencoffe, Béatrice Negulescu, Patrice Limelette, Jérôme Wolfman, et al.. Strain-induced resistance change in V_2O_3 films on piezoelectric ceramic disks. *Journal of Applied Physics*, 2019, 125 (11), pp.115102. 10.1063/1.5083941 . hal-02109266

HAL Id: hal-02109266

<https://hal.science/hal-02109266>

Submitted on 11 Feb 2022

HAL is a multi-disciplinary open access archive for the deposit and dissemination of scientific research documents, whether they are published or not. The documents may come from teaching and research institutions in France or abroad, or from public or private research centers.

L'archive ouverte pluridisciplinaire **HAL**, est destinée au dépôt et à la diffusion de documents scientifiques de niveau recherche, publiés ou non, émanant des établissements d'enseignement et de recherche français ou étrangers, des laboratoires publics ou privés.

Strain-induced resistance change in V_2O_3 films on piezoelectric ceramic disks

Cite as: J. Appl. Phys. **125**, 115102 (2019); <https://doi.org/10.1063/1.5083941>

Submitted: 02 December 2018 . Accepted: 04 March 2019 . Published Online: 19 March 2019

Joe Sakai , Maxime Bavencoffe , Beatrice Negulescu , Patrice Limelette , Jérôme Wolfman , Akinori Tateyama , and Hiroshi Funakubo 

COLLECTIONS

 This paper was selected as an Editor's Pick



View Online



Export Citation



CrossMark

Applied Physics Reviews
Now accepting original research

2017 Journal
Impact Factor:
12.894

AIP
Publishing

Strain-induced resistance change in V_2O_3 films on piezoelectric ceramic disks

Cite as: J. Appl. Phys. 125, 115102 (2019); doi: 10.1063/1.5083941

Submitted: 2 December 2018 · Accepted: 4 March 2019 ·

Published Online: 19 March 2019



Joe Sakai,^{1,a),b)} Maxime Bavencoffe,¹ Beatrice Negulescu,¹ Patrice Limelette,¹ Jérôme Wolfman,¹ Akinori Tateyama,² and Hiroshi Funakubo²

AFFILIATIONS

¹GREMAN, UMR 7347 CNRS/Université de Tours/INSA-CVL, Parc de Grandmont, 37200 Tours, France

²Tokyo Institute of Technology, 4259 Nagatsuta-cho, Midori-ku, Yokohama 226-8502, Japan

^{a)}Present address: ICN2, Campus de la UAB, 08193 Bellaterra, Spain.

^{b)}E-mail: sakai.joe@gmail.com

ABSTRACT

We prepared a stacked structure consisting of a quasi-free-standing functional oxide thin film and a ceramic piezoelectric disk and observed the effect of the piezoelectric disk deformation on the resistance of the thin film. Epitaxial V_2O_3 films were grown by a pulsed laser deposition method on muscovite mica substrates, peeled off using Scotch tapes, and transferred onto piezoelectric elements. In this V_2O_3 /insulator/top electrode/piezoelectronic disk/bottom electrode structure, the resistance of the V_2O_3 film displayed a variation of 60% by sweeping the piezoelectronic disk bias. With support from x-ray diffraction measurements under an electric field, a huge gauge factor of 3×10^3 in the V_2O_3 film was inferred. The sizeable resistance change in the V_2O_3 layer is ascribed to the piezo-actuated evolution of c/a ratios, which drives the material towards an insulating phase. A memory effect on the resistance, related to the hysteretic displacement of the piezoelectric material, is also presented.

Published under license by AIP Publishing. <https://doi.org/10.1063/1.5083941>

I. INTRODUCTION

Among the various materials whose physical properties are strain dependent, vanadium sesquioxide (V_2O_3) has been of great interest for half a century because of its rich temperature-pressure phase diagram. It consists of three phases, namely, paramagnetic metal (PM), paramagnetic insulator (PI), and antiferromagnetic insulator (AFI).¹ Pure V_2O_3 is in the PM phase at room temperature (RT) and under atmospheric pressure. Cr-doping converts the material into a PI phase in the same conditions, while the PM phase is recovered by applying hydrostatic pressure to Cr-doped V_2O_3 . This reversible conversion from metallic to insulating phases and *vice versa* can be described with respect to the negative and positive pressure, respectively. It is also known that the c/a ratio of V_2O_3 jumps at the transition, i.e., c/a is high (>2.815) in the PM phase, while it is low (<2.79) in the PI phase,^{2,3} suggesting that the electrical properties of V_2O_3 are closely related to its strain. In a previous work, we prepared a series of V_2O_3 films on sapphire substrates with various deposition conditions, resulting in a wide range of c/a ratios. Their physical properties, such as the PM–AFI phase transition temperature

and resistivity ratio between high and low temperatures, were revealed to be clearly dependent on the c/a ratio at RT.⁴ The tendency was that the PM–AFI transition temperature is higher in films with a lower c/a ratio at RT, indicating the stabilization of the insulating phase, and was qualitatively consistent with the change of c/a ratio at the phase transition reported in bulk materials. This behavior suggests that one can expect to drive the V_2O_3 material from a metallic regime to an insulating one by artificially controlling its c/a ratio. Preparing the material in a thin film form, especially in an epitaxial manner on a single crystal substrate, is convenient in order to realize a huge strain. However, in order to apply the mechanism to devices, the c/a ratio must be modified *in situ*.

Some ideas for the *in situ* strain-induced conductivity control of V_2O_3 have been reported. Newns *et al.* have proposed a piezoelectronic transistor, in which a piezoelectric layer and a so-called piezoresistive layer are confined in a rigid frame. Its operation principle is that the electric conductance in the piezoresistive layer is tuned through its strain by means of mechanical stress applied from the electrically-driven piezoelectronic layer. Cr-doped V_2O_3 was listed as one of the candidate materials for the piezoresistive

layer in their proposal.⁵ Recently, we have used a conductive atomic force microscopy (C-AFM) system to apply a local pressure of sub-gigapascal to a c axis-oriented V_2O_3 film and achieved obvious metal-insulator transition.⁶ These two configurations are categorized as the approaches in which an external stress is applied along the out-of-plane direction to a film. In the present work, we attempted to apply an in-plane external stress to a V_2O_3 film. The structure simply consists of a quasi-free-standing V_2O_3 film fixed on an M-I-M-structured piezoelectric element, with neither a rigid frame nor an AFM tip. Such a design was inspired by a number of previous studies on strain-induced modification of magnetic properties of thin films placed on piezoelectric bases.^{7–12} Driving the phase-change properties of VO_x by the piezoelectric force has also been reported, mainly in VO_2 films directly deposited on $Pb(Mg_{1/3}Nb_{2/3})O_3$ - $PbTiO_3$ (PMN-PT) single crystal substrates.^{13–15} Nevertheless, no study on the combination of a VO_x film and a low-cost polycrystalline piezoelectric element has been reported so far.

The V_2O_3 film used in the present experiment should be single-oriented (most simply, c axis-oriented) in order to obtain the maximum strain effect. However, the commercially-available low-cost piezoelectric disks are made of polycrystalline ceramics with multi-oriented grains, meaning almost no chance for the V_2O_3 layer to grow single-oriented directly on it. One possible strategy to obtain a single-oriented film on a polycrystalline substrate is to place a free-standing crystalline buffer layer on the desired substrate and then grow the desired film.^{16–18} Another may be to epitaxially grow the desired film on a layered-structured crystalline substrate that is then peeled off and transferred onto the desired substrate. In this work, we adopted the latter strategy due to its simplicity. Mica was chosen as the substrate material because of its layered structure that is easily exfoliated with an adhesive tape (often referred to as a “Scotch tape method”). The in-plane lattices of both muscovite mica and V_2O_3 are regarded as quasi-hexagonal structures, with lattice parameters a of 5.19 and 4.95 Å, respectively,^{19,20} giving a lattice mismatch of about 5%. In samples with a stacked structure of V_2O_3 /insulator/top electrode/piezoelectric disk/bottom electrode, we measured the resistance of the V_2O_3 layer ($R_{V_2O_3}$) as a function of the piezoelectric disk bias (V_p). As a result, we observed a sizeable variation of $R_{V_2O_3}$ that can only be explained by the resistivity change due to the piezo-induced modification of its c/a .

II. EXPERIMENTAL DETAILS

A. Films deposition process and crystallographic characterization

V_2O_3 films were deposited onto muscovite mica substrates by means of a pulsed laser deposition (PLD) method using a ceramic V_2O_5 target. Deposition conditions such as Ar ambient pressure (2×10^{-2} mbar), repetition rate and deposition duration of the KrF excimer laser (Lambda Physik, COMPex 102; 5 Hz, 1800s), input energy, and fluence on the target surface (65 mJ, 2.0 J/cm²) are the same as those for V_2O_3 deposition on sapphire substrates previously reported.⁴ Only the substrate temperature was set lower (575 °C) considering a low melting temperature of mica. TiN_x layers for a control experiment were deposited on the muscovite mica substrates with a reactive dc sputtering method using a Ti target in an N_2 gas

ambient of 5 mTorr. All the films for the $R_{V_2O_3}$ - V_p experiments were deposited through a shadowing mask to pattern strips.

X-ray diffraction (XRD; Bruker, D8) measurements such as 2θ - ω , ϕ -scans, and reciprocal space mapping (RSM) were performed for non-patterned V_2O_3 films with Cu K α radiation. The thickness of the V_2O_3 film on mica was assumed to be identical to that of a V_2O_3 film deposited in the same run on a C-plane sapphire substrate, whose 2θ - ω profile contained Laue fringes that allow deducing its thickness. XRD 2θ - ω scans with a bias voltage to the piezoelectric disk were performed on a V_2O_3 film/thin mica/piezoelectric element stacked sample. The piezoelectric element was fixed on a glass plate with pieces of Scotch tape. Sample alignment along z (height), ω , and χ (tilting) axes was performed after every voltage change (at $\omega \sim 0^\circ$ for the z axis, while around $2\theta \sim 45.4^\circ$, a strong diffraction peak from mica, for ω and χ axes).

B. Transferring the film to the piezoelectric disk

The V_2O_3 layer, with a thin layer of mica, was exfoliated from the mica substrate and transferred to a commercial lead zirconate titanate (PZT)-based piezoelectric element by a Scotch tape. Prior to the transferring, Au (200 nm)/Ti (20 nm) electrode pads for a four-probe measurement were deposited on the V_2O_3 strips by a dc sputtering method using a shadowing mask [Fig. 1(i)]. The V_2O_3 film was peeled off of the mica substrate by a removable-type Scotch tape [Fig. 1(ii)], and pasted onto a commercial piezoelectric element (SPL, SPT08) with cyanoacrylate glue [Fig. 1(iii)]. The piezoelectric element consists of a 0.2 mm-thick PZT-based piezoelectric disk, a 0.2 mm-thick metal plate as the bottom electrode, and a nickel (Ni) thin film as the top electrode. The layered structure of mica allows one to easily peel off the deposited layer, which is, however, inevitably accompanied by a very thin mica layer. This thin mica layer plays the

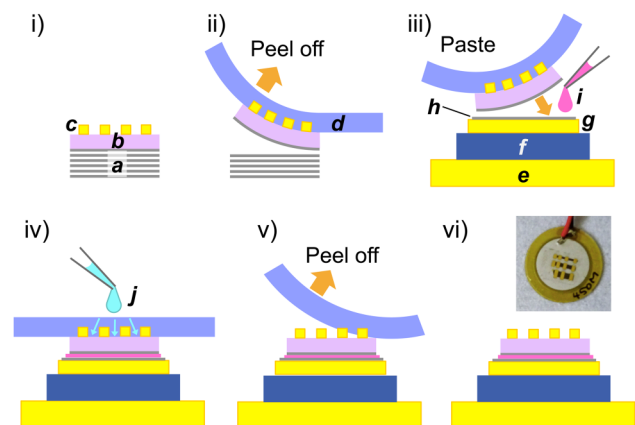


FIG. 1. Schematic of the transferring process of a V_2O_3 thin film from a mica substrate to a piezoelectric element. (a) Mica substrate, (b) V_2O_3 , (c) Au/Ti electrodes, (d) removable-type Scotch tape, (e)–(g) piezoelectric element where a 0.2 mm-thick piezoelectric disk (f) is sandwiched by the bottom electrode [0.2 mm-thick metallic plate (e)] and the top electrode [Ni film (g)], (h) thin mica layer for insulation, (i) cyanoacrylate glue, (j) ethanol. Inset photograph shows the finished sample.

role of an insulator that prevents the electrical contact between the piezoelectric transducer and the V_2O_3 sample, still we pasted another thin mica layer larger than the V_2O_3 sample on the top electrode to ensure the insulation [h in Fig. 1(iii)]. After the glue is dried, a drop of ethanol was added onto the tape. Thanks to the porous structure of the removable-type Scotch tape, the liquid can penetrate to the back side of the tape, where it selectively dissolves the glue of the tape without affecting the cyanoacrylate glue [Fig. 1(iv)]. Thus, the tape can be removed [Fig. 1(v)], leaving the V_2O_3 film on the piezoelectric disk [Fig. 1(vi)].

C. Electrical and mechanical properties measurement

V_p dependence of $R_{V_2O_3}$ ($R_{V_2O_3}-V_p$) in the stacked samples was measured in air at RT. For the four-probe resistance measurement, a constant current was provided by a dc power source (Yokogawa, 7651) and the voltage on the film was recorded by a data logger (Graphtec, GL820). Sinusoidal bias was generated by a function/arbitrary waveform generator (Agilent, 33250A) and provided to the piezoelectric disk after 200-times amplified by a high voltage power amplifier (TREK, PA05039) to achieve the amplitude of 200 V at maximum. The current for resistance measurement was $50 \mu A$ (V_2O_3) and 1 mA (TiN_x). The frequency of V_p was 0.1 Hz. In the case of memory effect measurement, the bias was provided to the disk by a dc high-voltage source (Keithley, 2410).

The piezoelectric coefficient d_{33} of the element (of the same product number but a different chip from samples in the main experiments) was measured as a function of bias by using a laser Doppler vibrometer (Polytec, OFV-552 and OFV-3001). A small wave (of an amplitude of 10 V and a frequency of 1 kHz) was superposed over a large wave (of 250 V and 0.1 Hz), and then the response was collected through a lock-in amplifier. Out-of-plane strain as a function of V_p was obtained by multiplying d_{33} by V_p . The in-plane strain of the piezoelectric element was measured with a strain gauge (Tokyo Measuring Instruments Lab., CFLA-1-350-17) pasted on it with cyanoacrylate glue. Each resistance value of the gauge was recorded after being stabilized.

III. RESULTS AND DISCUSSION

XRD analysis of the obtained V_2O_3 films on the mica substrates revealed that the films were out-of-plane oriented along its c -axis [Fig. 2(a)] and in-plane oriented in sixfold symmetry [Fig. 2(b)], suggesting the epitaxial growth of the films. The c -axis lattice parameter of a V_2O_3 layer was found from the $2\theta-\omega$ profile to be 13.97 Å, indicating slight out-of-plane compressive strain. RSM around V_2O_3 (1 0 10) reflection [Fig. 2(c)] has revealed broadening of the a -axis parameter approximately from 4.8 to 5.2 Å, bridging two specific c/a regions, one ($c/a < 2.79$) corresponding to the insulating phase in bulks, and the other ($c/a > 2.815$) corresponding to the metallic phase. The film may contain components of both phases, although the stronger signals are from the low c/a region.

Figure 3(a) shows the results of $R_{V_2O_3}-V_p$ properties in a ~ 50 nm-thick V_2O_3 film, where V_p was swept sinusoidally with various amplitudes ($V_{p,amp}$) from 50 to 200 V. The resistance value at zero bias (R_0) of around 200 Ω, which corresponds to a resistivity of the order of 10^{-4} Ω cm, suggests the existence of a metallic phase of the V_2O_3 film at RT.⁴ The formation of a filament-like conductive

path could explain the coexistence of the component of low resistivity and that of low c/a found in the RSM. In a region of $V_{p,amp} \leq 90$ V (corresponding to the electric field ≤ 4.5 kV/cm), $R_{V_2O_3}$ increases monotonically as V_p increases, indicating the strain-induced modification of the electric property of the film. At a certain $V_{p,amp}$, the shape of $R_{V_2O_3}-V_p$ curves transforms from monotonous to butterfly-type, which contains a sudden drop of the resistance during the increase of bias. The transformation from monotonous

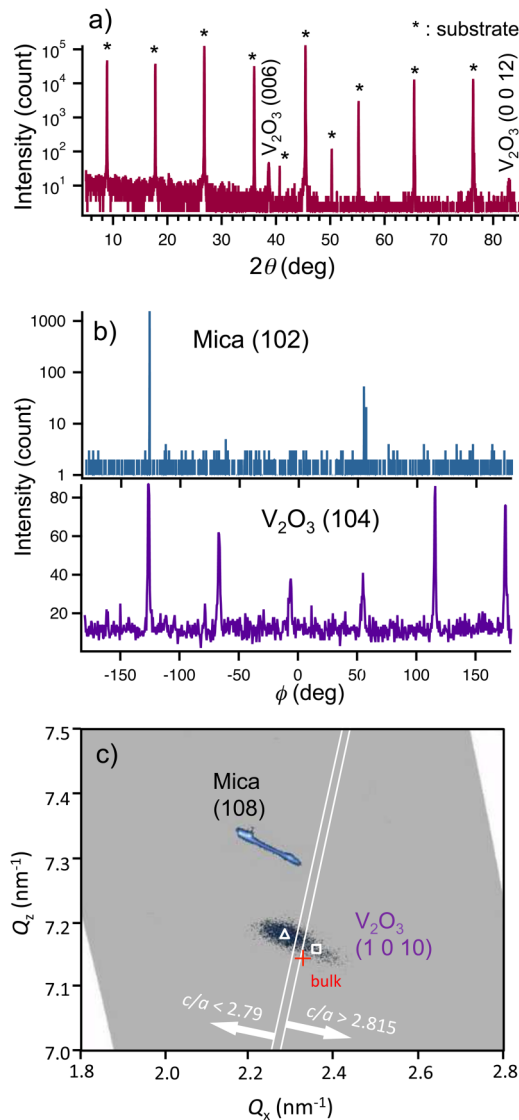


FIG. 2. XRD results from a V_2O_3 /muscovite mica sample. (a) $2\theta-\omega$ profile. (b) ϕ -scan profiles around the mica (102) peak (top) and the V_2O_3 (104) peak (bottom). (c) A RSM image around the mica (108) and the V_2O_3 (1 0 10) reflections. Two white lines represent c/a ratios of 2.79 and 2.815. Triangle and square symbols, corresponding to (a, c) of (5.1 Å, 13.9 Å) and (4.9 Å, 14.0 Å), respectively, represent centers of two typical components.

to butterfly-type occurred gradually between 90 and 100 V of amplitude [see inset of Fig. 3(a)]. With a $V_{p \text{ amp}}$ of 200 V, the maximum resistance and the minimum resistance during the cycling (276.8 and 157.0 Ω , respectively) give the peak-to-peak resistance change (ΔR) of 119.8 Ω , reaching 60% of R_0 (199.0 Ω). Naturally, when the $R_{V_2O_3} - V_p$ curves are of butterfly-type, the peak of resistance appears twice in a cycle of V_p , suggesting a possibility to utilize the present system as a frequency doubler that can be switched on/off by the voltage (Fig. 4). We performed a control experiment on another sample with the same structure but with a ~ 100 -nm-thick TiN_x layer instead of V_2O_3 . The result is shown in Fig. 3(b), with the monotonous or the butterfly-type curves quite similar to those in the V_2O_3 sample, suggesting a common driving force for the resistance change in both V_2O_3 and TiN_x . Nevertheless, only a feeble resistance change ratio $\Delta R/R_0$ of 0.7% was observed on the TiN_x layer. The hundred times-higher relative

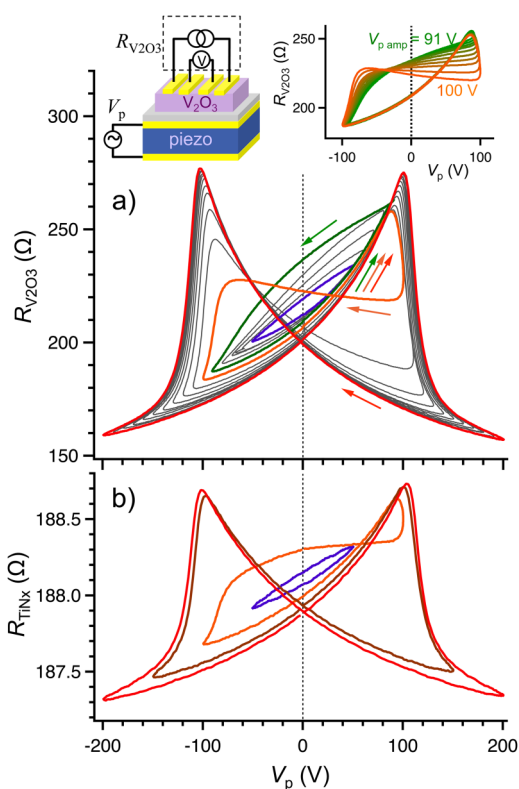


FIG. 3. (a) Resistance of the V_2O_3 layer ($R_{V_2O_3}$) on the piezoelectric element as a function of piezoelectric bias (V_p). Bias amplitude ($V_{p \text{ amp}}$) was varied from 50 to 200 V with an increment of 10 V. Inset shows a schematic illustration of V_2O_3 /piezoelectric element stacked sample with the measurement setup, and an enlarged view of $R_{V_2O_3} - V_p$ curves for $V_{p \text{ amp}}$ from 91 to 100 V with an increment of 1 V. (b) Resistance of a TiN_x layer on the piezoelectric element as a function of V_p . $V_{p \text{ amp}}$ was varied from 50 to 200 V with an increment of 50 V. The width of the V_2O_3 strip in (a) and the TiN_x strip in (b) was 0.5 mm and 1.5 mm, respectively. Distance between two voltage electrodes was 1.0 mm for both cases.

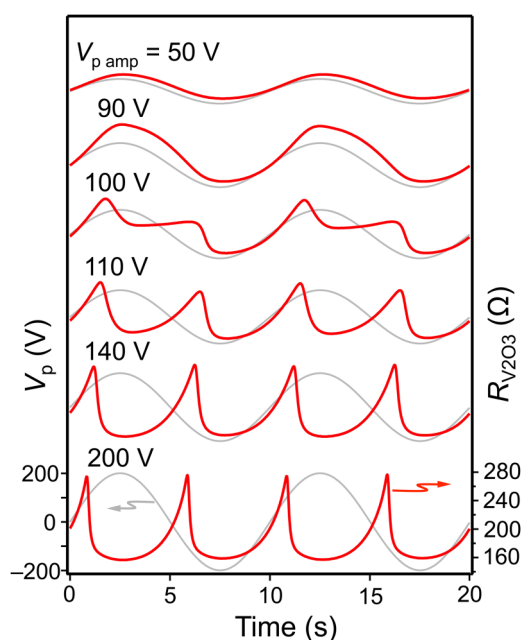


FIG. 4. Resistance of V_2O_3 (right scale) and piezoelectric bias (left scale) as functions of time, with various amplitudes of piezoelectric bias.

variation of resistance in V_2O_3 indicates an anomalously high strain dependence of resistivity.

The observed $R_{V_2O_3} - V_p$ behaviors, the monotonous increase with a hysteresis for small $V_{p \text{ amp}}$ and the butterfly-type curves for large $V_{p \text{ amp}}$, are similar to the usual minor and major loop deformation curves of piezoelectric materials. Figures 5(a) and 5(b) show out-of-plane strain (ϵ_{out}) and in-plane strain (ϵ_{in}), respectively, of the piezoelectric element as functions of V_p . The butterfly piezoelectric cycle is observed when the electric field is large enough to induce the polarization reversal. A smaller ϵ_{out} than the expected one for pristine PZT (0.25% p-p in present result against 0.4% p-p in pristine one)^{21,22} is probably due to restriction by the bottom electrode plate. As the piezoelectric disk expands in the out-of-plane direction, there is a correlated in-plane contraction, i.e., the piezoelectric disk exerts an in-plane compressive strain on the V_2O_3 film, which in turn results in the elongation of the c -axis and the shrinkage of the a -axis and thus an increase of the V_2O_3 c/a ratio. Conversely, the out-of-plane deformation of the piezo disk vanishes at the coercive field, as well as the in-plane compressive strain exerted on V_2O_3 , leading to a decrease of the V_2O_3 c/a ratio. This strongly suggests that the change of $R_{V_2O_3}$ is induced by the deformation of the piezoelectric disk, as the insulating (metallic) phase of V_2O_3 is accompanied by a low (high) c/a ratio.

To evaluate the out-of-plane piezo-driven strain of the mica layer, we performed XRD $2\theta - \omega$ scans applying various V_p . V_p of -200 V was applied prior to the measurement, followed by the measurement with V_p changed as $0 \rightarrow +100 \rightarrow 0 \rightarrow -200$ V, expecting negative poling throughout the measurement. We observed the apparent shift of the mica (005) diffraction peak,

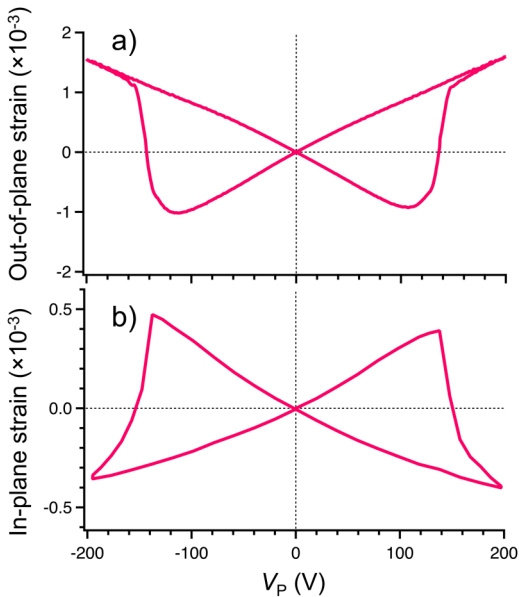


FIG. 5. Out-of-plane (a) and in-plane (b) strain of the piezoelectric element as functions of V_p . The out-of-plane displacement was calculated by multiplying d_{33} by V_p . The in-plane strain was obtained from a strain gauge pasted on the element.

depending on the history of V_p [Fig. 6(a)]. As shown in Fig. 6(b), ϵ_{out} of the mica layer displays a normal tendency, shrinking under a positive bias (+100 V) and retaining a part of deformation (0 V) compared to the initial zero-bias state. Nevertheless, ϵ_{out} in the mica layer at +100 V (-4.5×10^{-5}) was as small as one-tenth of ϵ_{in} in the piezoelectric layer [4×10^{-4} ; Fig. 5(b)]. This suggests that the transfer of the piezoelectric base in-plane deformation toward the mica layer is incomplete, probably due to some elastic deformation of the glue in-between. We attempted to estimate the gauge factor (γ) of the V_2O_3 layer by using the above results, assuming that ϵ_{in} is identical between the mica layer and the V_2O_3 film deposited on it. Under 2d isotropic stress applied in-plane, ϵ_{in} and ϵ_{out} are related as $\epsilon_{\text{in}} = (-1/2\nu) \epsilon_{\text{out}}$, where ν is Poisson's ratio, 0.25 for mica.²⁵ $\Delta R/R_0$ of $\sim 30\%$ [Fig. 3(a)] and ϵ_{out} (mica) of $\sim 4.5 \times 10^{-5}$ [Fig. 6(b)] for $0 \leq V_p \leq +100$ V give a γ , defined as $(\Delta R/R_0)/\epsilon_{\text{in}}$, of the V_2O_3 layer of 3.3×10^3 . This value is outstanding compared to γ of general metal thin films in a range of 10^0 – 10^2 .^{23,24} The only explanation for the huge γ of the V_2O_3 layer should be the piezo-actuated evolution of c/a ratios, which drove the material towards insulating phase, even though the initial c/a ratios have been scattered in a wide range. The present mechanism is expected to offer even more significant resistivity change, if the in-plane deformation of a pristine piezoelectric base could be 100% transferred to the V_2O_3 layer (in which case ϵ_{in} of V_2O_3 would be about 15 times larger than the present experiment). Further study should be focused on improving the strength of displacement in the piezoelectric layer and the stress transfer efficiency between piezoelectric and V_2O_3 layers.

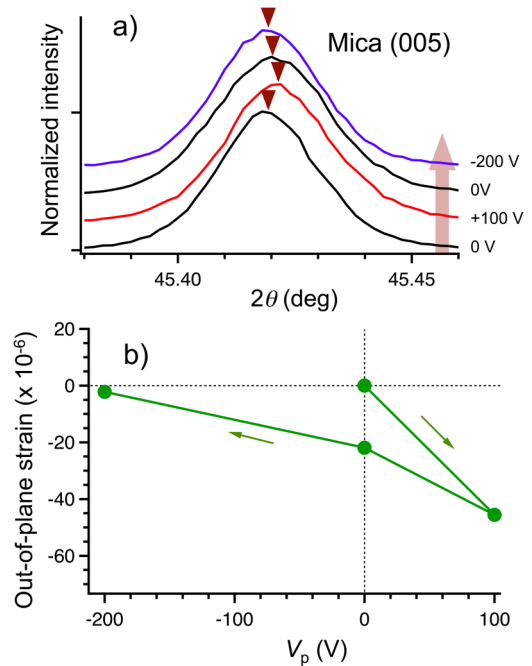


FIG. 6. (a) 2θ - ω profiles around the mica (005) reflection in a V_2O_3 film/thin mica layer/piezoelectric element stacked sample with application of V_p as $0 \rightarrow +100 \rightarrow 0 \rightarrow -200$ V. The piezoelectric layer was negatively poled prior to the measurement. Intensity is normalized. Triangles indicate the center of peaks deduced from fitting with a pseudo-Voigt function. (b) Evolution of out-of-plane strain, calculated from the XRD peak position in (a), of the mica layer along the change of V_p .

Finally, we mention the memory effect of the present sample. As one can see in the hysteretic minor loops in Fig. 3(a), $R_{V_2O_3}$ can take different values at zero bias ($V_p = 0$), depending on the history of V_p . Figure 7(a) shows V_p and $R_{V_2O_3}$ as the functions of time, in which V_p was manually controlled. We find that $R_{V_2O_3}$ at zero bias (which we define as “memory resistance”) retained at various values after various V_p (“set voltage”), suggesting its function as a multi-level resistive random access memory (ReRAM) or a memristor. Retention of the memory resistance for a long period as 7000 s was also confirmed [Fig. 7(a)]. Figure 7(b) shows the relationship between the set voltage and the memory resistance, showing that the memory resistance is a monotonous function of the set voltage as far as the piezoelectric layer retains the negative poling. The memory resistance in Fig. 7(b) ranged from 210.0 to 235.2 Ω , i.e., it varied for 12% with respect to its minimum value. The origin of this feeble memory effect is, most likely, the hysteresis in deformation of the piezoelectric disk. On the other hand, the PI-PM phase transition is known to be of the first order, and thus the evolution of the resistance according to the hydrostatic pressure contains a hysteresis region.²⁶ Therefore, one can expect a strain-induced non-volatile resistance switching between PM and PI phases (=a memory effect) on a V_2O_3 -based material with a huge resistance change of three orders of

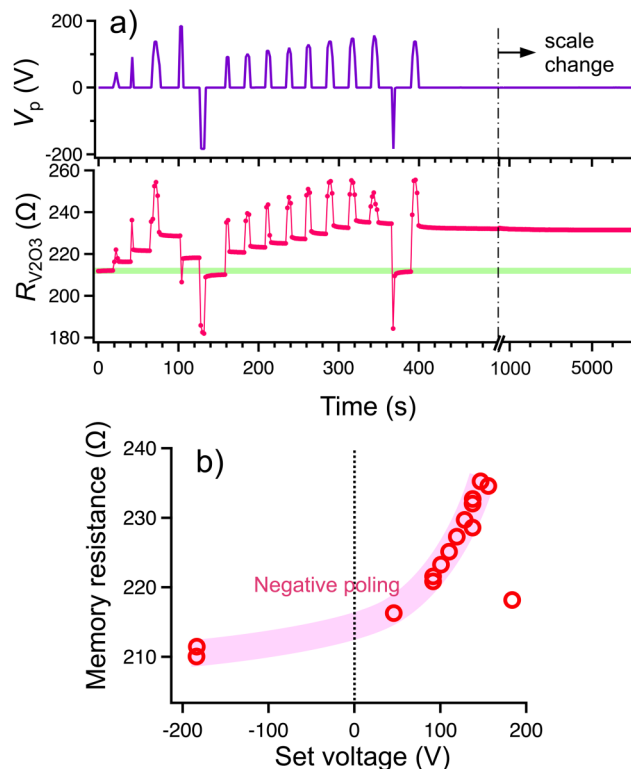


FIG. 7. (a) V_p (top) and $R_{V_2O_3}$ (bottom) as the functions of time, in which V_p was manually controlled. The horizontal thick line represents the $R_{V_2O_3}$ at zero-bias after setting V_p at -200 V. (b) Plots of the memory resistance and the set voltage. The thick curve indicates the group of data points after negative poling.

magnitude.² Advantageously, the memory effect based on the PM–PI phase transition in V_2O_3 is expected to work at the whole temperature region of this boundary, from 180 K to 390 K,² well covering the required operating temperatures of both commercial and industrial devices.

IV. CONCLUSIONS

We grew epitaxial (0001)-oriented V_2O_3 thin films by a PLD technique on muscovite mica substrates and then transferred a peeled-off V_2O_3 film onto a commercial ceramic PZT-based piezoelectric element. The $R_{V_2O_3}$ – V_p property on this sample showed butterfly-type curves that reflected the deformation of the piezoelectric disk. The 60% peak-to-peak change of $R_{V_2O_3}$ and the ϵ_{out} of the mica layer, detected by a biased XRD technique, allowed one to roughly estimate a huge gauge factor of this V_2O_3 film to be about 3×10^3 , ascribed to the piezo-actuated evolution of c/a ratios. A multi-level memory effect related to the hysteretic deformation of the piezoelectric disk was observed in the $R_{V_2O_3}$ – V_p

properties. The bilayer of piezoresistive and piezoelectric materials offers a possibility of piezoelectrically-driven switching and memory devices with simple structures.

ACKNOWLEDGMENTS

This work was financially supported by Région Centre, France, through Project COMHET (No. 2013 00082885). J.S. appreciates Fabien Pierre at STMicroelectronics Tours for providing muscovite mica substrates.

REFERENCES

- ¹D. B. McWhan, A. Menth, J. P. Remeika, W. F. Brinkman, and T. M. Rice, *Phys. Rev. B* **7**, 1920 (1973).
- ²D. B. McWhan and J. P. Remeika, *Phys. Rev. B* **2**, 3734 (1970).
- ³F. Rodolakis, J. P. Rueff, M. Sikora, I. Alliot, J. P. Itié, F. Baudelet, S. Ravy, P. Wzietek, P. Hansmann, A. Toschi, M. W. Haverkort, G. Sangiovanni, K. Held, P. Metcalf, and M. Marsi, *Phys. Rev. B* **84**, 245113 (2011).
- ⁴J. Sakai, P. Limelette, and H. Funakubo, *Appl. Phys. Lett.* **107**, 241901 (2015).
- ⁵D. Newns, B. Elmegreen, X. H. Liu, and G. Martyna, *J. Appl. Phys.* **111**, 084509 (2012).
- ⁶N. Alyabyeva, J. Sakai, M. Bavencoffe, J. Wolfman, P. Limelette, H. Funakubo, and A. Ruyter, *Appl. Phys. Lett.* **113**, 241603 (2018).
- ⁷H. J. A. Molegraaf, J. Hoffman, C. A. F. Vaz, S. Gariglio, D. van der Marel, C. H. Ahn, and J.-M. Triscone, *Adv. Mater.* **21**, 3470 (2009).
- ⁸A. Brandlmaier, S. Geprägs, G. Woltersdorf, R. Gross, and S. T. B. Goennenwein, *J. Appl. Phys.* **110**, 043913 (2011).
- ⁹R. K. Zheng, Y. Wang, Y. K. Liu, G. Y. Gao, L. F. Fei, Y. Jiang, H. L. W. Chan, X. M. Li, H. S. Luo, and X. G. Li, *Mater. Chem. Phys.* **133**, 42 (2012).
- ¹⁰S. Zhang, Y. G. Zhao, P. S. Li, J. J. Yang, S. Rizwan, J. X. Zhang, J. Seidel, T. L. Qu, Y. J. Yang, Z. L. Luo, Q. He, T. Zou, Q. P. Chen, J. W. Wang, L. F. Yang, Y. Sun, Y. Z. Wu, X. Xiao, X. F. Jin, S. Zhang, Y. G. Zhao, P. S. Li, J. J. Yang, S. Rizwan, J. X. Zhang, J. Seidel, T. L. Qu, Y. J. Yang, Z. L. Luo, Q. He, T. Zou, Q. P. Chen, J. W. Wang, L. F. Yang, Y. Sun, Y. Z. Wu, X. Xiao, X. F. Jin, J. Huang, C. Gao, X. F. Han, and R. Ramesh, *Phys. Rev. Lett.* **108**, 137203 (2012).
- ¹¹P. M. Leufke, R. Kruk, R. A. Brand, and H. Hahn, *Phys. Rev. B* **87**, 094416 (2013).
- ¹²A. T. Chen and Y. G. Zhao, *APL Mater.* **4**, 032303 (2016).
- ¹³T. Nan, M. Liu, W. Ren, Z. G. Ye, and N. X. Sun, *Sci. Rep.* **4**, 5931 (2014).
- ¹⁴A. Petraru, R. Soni, and H. Kohlstedt, *Appl. Phys. Lett.* **105**, 092902 (2014).
- ¹⁵B. Zhi, G. Gao, H. Xu, F. Chen, X. Tan, P. Chen, L. Wang, and W. Wu, *Appl. Mater. Interfaces* **6**, 4603 (2014).
- ¹⁶H. Ohta, A. Muzutani, K. Sugiura, M. Hirano, H. Hosono, and K. Koumoto, *Adv. Mater.* **18**, 1649 (2006).
- ¹⁷T. Shibata, H. Takano, Y. Ebina, D. S. Kim, T. C. Ozawa, K. Akatsuka, T. Ohnishi, K. Takada, T. Kogure, and T. Sasaki, *J. Mater. Chem. C* **2**, 441 (2014).
- ¹⁸D. Lu, D. J. Baek, S. S. Hong, L. F. Kourkoutis, Y. Hikita, and H. Y. Hwang, *Nat. Mater.* **15**, 1255 (2016).
- ¹⁹L. Sun, P. C. Searson, and C. L. Chien, *Appl. Phys. Lett.* **74**, 2803 (1999).
- ²⁰M. G. Vincent, K. Yvon, and J. Ashkenazi, *Acta Crystallogr.* **A36**, 808 (1980).
- ²¹K. Uchino, *Am. Ceram. Soc. Bull.* **65**, 647 (1986).
- ²²M. H. Malakooti and H. A. Sodano, *Appl. Phys. Lett.* **102**, 061901 (2013).
- ²³G. C. Kuczynski, *Phys. Rev.* **94**, 61 (1954).
- ²⁴R. L. Parker and A. Krinsky, *J. Appl. Phys.* **34**, 2700 (1963).
- ²⁵G. Zhang, Z. Wei, and R. E. Ferrell, *Appl. Clay Sci.* **43**, 271 (2009).
- ²⁶P. Limelette, A. Georges, D. Jérôme, P. Wzietek, P. Metcalf, and J. M. Honig, *Science* **302**, 89 (2003).